

O. SILVESTRE<sup>1</sup>  
M.C. PUJOL<sup>1,✉</sup>  
F. GÜELL<sup>1</sup>  
M. AGUILÓ<sup>1</sup>  
F. DÍAZ<sup>1</sup>  
A. BRENIER<sup>2</sup>  
G. BOULON<sup>2</sup>

## Crystal growth and spectroscopic analysis of codoped (Ho,Tm):KGd(WO<sub>4</sub>)<sub>2</sub>

<sup>1</sup> Física i Cristal·lografia de Materials (FiCMA), Universitat Rovira i Virgili, Campus Sescelades c/Marcel·lí Domingo, s/n, 43007 Tarragona, Spain  
<sup>2</sup> Physico Chimie des Matériaux Luminescents, Université Claude Bernard Lyon 1, UMR 5620 CNRS, Bât. A. Kastler, 10 rue Ampère, 69622 Villeurbanne Cedex, France

Received: 24 August 2006

Published online: 24 November 2006 • © Springer-Verlag 2006

**ABSTRACT** We present the crystal growth of monoclinic KGd(WO<sub>4</sub>)<sub>2</sub> codoped with holmium and thulium by a top-seeded solution growth and slow cooling method. Macrodefect-free crystals with sizes about  $8.5 \times 5 \times 12$  ( $a^* \times b \times c$ , dimensions in mm) were obtained. A complete study of the spectroscopic parameters of the holmium emission  $^5I_7 \rightarrow ^5I_8$ , around 2 microns, sensitized by the thulium ion, was made. Polarized absorption measurements were performed to characterize the optimum pumping wavelength in the system. The maximum value of the cross section is  $8.0 \times 10^{20}$  cm<sup>2</sup> with  $E//N_p$  direction at a wavelength value of 794 nm. The emission cross section of the 2-micron holmium transition has been calculated by the reciprocity method. The experimental lifetime of the  $^5I_7$  level has been measured in relation to holmium and thulium concentrations.

**PACS** 81.10.-h; 42.55.Rz; 78.55.-m

### 1 Introduction

The importance of the 2-micron laser emission wavelength lies in the fact that the fundamental symmetric and asymmetric vibronic stretching mode of water molecules (2.94  $\mu$ m) and the harmonic (1.94  $\mu$ m) absorb this laser emission [1]. The application of lasers of around 2 microns in medicine involving coagulating and welding makes it important to enhance research into laser media in this eye-safe range. Moreover, these lasers are also used in radar applications and remote sensing such as diode-pumped 2- $\mu$ m LIDAR transmitters for wind measurements [2].

The first report of room-temperature cw laser operation of 2  $\mu$ m pumped by a diode laser in a thulium-doped material was in Tm<sup>3+</sup>:YAG based on the electronic transition  $^3F_4 \rightarrow ^3H_6$  by Braud et al. in 1995 [3]. Some years before, the 2-micron laser emission was achieved using holmium as the active ion with the electronic transition  $^5I_7 \rightarrow ^5I_8$  in Ho:YAG by Stoneman and Esterowitz in 1992 [4] and in a codoped system by Fan et al. in 1988 [5]. Within the family of monoclinic double tungstates, the first report of thulium laser emission in this range of wavelengths was in 1997 in Tm<sup>3+</sup>:KGd(WO<sub>4</sub>)<sub>2</sub>

(hereafter KGdW) rods sensitized with Er<sup>3+</sup> and Yb<sup>3+</sup> at 1.92 and 1.93 microns by a Xe flash lamp at cryogenic temperatures [6] and the first report of holmium codoped tungstate was in 1977 by Kaminskii et al. [7]. The Ho<sup>3+</sup> laser channel at 2.072  $\mu$ m in KGdW was demonstrated in [8].

Holmium–thulium codoped crystals are well known as efficient 2-micron-range laser systems. The efficiency of the thulium sensitizer–holmium active ion couple is based on the fact that, though the holmium ion is not very suitable to be pumped by commercially available diodes, both the fact that the absorption cross section of  $^3H_6 \rightarrow ^3H_4$  (Tm<sup>3+</sup>) is higher than that of the holmium absorption cross section and the thulium quantum efficiency, 2, due to the cross-relaxation mechanism ( $^3H_4 + ^3H_6$ )  $\rightarrow$  ( $^3F_4 + ^3F_4$ ) mean that these codoped systems are interesting alternatives to the single-doped systems. Population in the energy transfer manifold,  $^3H_4$ , can also come from two other cross-section mechanisms, ( $^3H_4, ^3H_6$ )  $\rightarrow$  ( $^3H_5, ^3F_4$ ) and ( $^3H_4, ^3H_6$ )  $\rightarrow$  ( $^3F_4, ^3H_5$ ) [9]. Also, the gain for holmium  $^5I_7 \rightarrow ^5I_8$  transitions is several times larger than for thulium  $^3F_4 \rightarrow ^3H_6$  emission. Another difference compared to a direct-pumped laser system such as Tm or Ho is that, in the (Ho, Tm) system, the active Ho<sup>3+</sup> ions are excited through energy transfer, not by direct absorption of pump photons. With regard to the laser dynamics, external perturbations can be injected into the laser system by pump-power fluctuations. In (Ho, Tm) systems, therefore, in the pumping process, the two intermediate steps of cross relaxation and energy transfer can act as a low-pass filter on the original fluctuations of the pump-photon flux [10].

Energy transfer between lanthanide ions has been extensively studied. This transfer can take place via several mechanisms: multipolar interaction, studied by Dexter in 1953 [11] and Förster in 1959 [12]; the exchange coupling mechanism, studied by Inokuti and Hirayama in 1965 [13]; phonon-assisted transfer, studied by Miyakawa and Dexter in 1970 [14]; the diffusion of energy between donor systems, studied by Yokota and Tanimoto in 1967 [15] (Burhstein also included the effects of diffusion between ions [16]); and, finally, a percolation theory studied by Payne et al. in 1992 in which diffusion takes place along a chain of sensitizer atoms and eventually ends on an active atom [17]. The energy transfer process in holmium–thulium codoped systems is between the  $^3F_4$  thulium manifold and the  $^5I_7$  holmium manifold. In the bibliography, the (Ho, Tm) mechanism has been modelled

✉ Fax: +34-977-55-95-63, E-mail: mariacinta.pujol@urv.cat

using an electric dipole mechanism [18] and its temperature dependence [19, 20].

To our knowledge, codoped holmium–thulium monoclinic double tungstates have not been reported. The recent success of the ytterbium tungstate diode pumped solid state laser in the field of 1-micron emission and thulium doped tungstates in 2-micron emission [21, 22] led us to study the possibility of using these materials as laser hosts for the thulium-sensitized holmium emission at 2 microns. Previous studies of the single-doped Ho [23] and the single-doped Tm tungstates [24, 25] are a strong basis for studying these codoped materials. In this paper we study the effect of codoping on the structure and, especially, on the spectroscopic properties such as stimulated emission cross section, upper state lifetime of the transition and absorption spectra for diode laser pumping.

## 2 Experimental details

The crystal growth device comprised a vertical cylindrical furnace with a Kanthal wire as a heater element, a controller/programmer (Eurotherm 903 P) and a thyristor. The control temperature was  $\pm 0.01$  K. The description of the top-seeded solution growth and slow cooling (TSSG-SC) method for growing double-tungstate single crystals used by our group has been explained in [26, 27].  $K_2W_2O_7$  was used as a solvent and the solution composition was 11.5% solute–88.5% solvent. The driving force of the growth procedure is supersaturation created by slow cooling the temperature of the system. Crystallization and growth take place on a seed located in the centre of the free surface of the solution – the coolest point in the system. The seed is a parallelepipedic piece of undoped KGdW oriented parallel to the  $b$  direction. The saturation temperature can be determined by observing the growth or dissolution of a KGdW seed in contact with the surface of the solution. The crystals were submerged in the solution and constantly rotated.

The electron probe microanalysis (EPMA) was conducted in CAMECA sx50 equipment. The analyser crystal used was LiF (lithium fluoride (200)). For the constitutional elements, K, W, Gd and O, undoped KGdW was used as standard reference. To measure holmium, we used the  $L\beta$  line and the REE2 standard (P&H Developments) and to measure thulium we used the  $L\alpha$  line and the same standard. The parameters of

the electron beam were an intensity of 40 nA and a current of 25 kV.

The unit-cell parameters of codoped samples (Ho,Tm):KGdW were obtained from X-ray powder diffraction analysis, using a Siemens D-5000 diffractometer (Bragg–Brentano parafocusing geometry and a vertical  $\theta$ – $\theta$  goniometer). The X-ray powder diffraction patterns were recorded at  $2\theta = 10$ – $70^\circ$ , size step =  $0.02^\circ$  and step time = 16 s.

The high anisotropy of the tungstates meant that it was necessary to measure optical absorption with polarized light parallel to the three principal optical axes of the crystal ( $N_g$ ,  $N_m$  and  $N_p$ ) [28]. The samples were cut and polished (by alumina powder up to 0.3 microns) to obtain polished faces parallel to the optical principal planes with optical quality. Polarized measurements therefore had to be taken using a Glan–Taylor prism to obtain parallelism between the electrical field of the radiation and the principal optical axes. We performed the polarized optical absorption of  $Ho^{3+}$  and  $Tm^{3+}$  ions at room temperature using a Cary Varian 500 spectrophotometer.

The room-temperature (RT) fluorescence spectra were recorded with  $90^\circ$  geometry using an optical parametric oscillator from BM Industries pumped by a frequency-tripled Nd:YAG laser from Coherent. The pump power was around  $350 \mu J/pulse$  with a pulse duration of 10 ns and a pulse repetition of 10 Hz. The pump beam was focused onto the sample surface in a spot with a diameter of a few hundred  $\mu m$ . Fluorescence was dispersed by a H25 Jobin-Yvon monochromator equipped with a 2- $\mu m$  blazed grating and captured by an InGaAs detector cooled at  $N_2$  cryogenic temperature (77 K) in the near-infrared range. The electronic signal was analysed by a Lecroy oscilloscope connected in parallel with a computer.

## 3 Crystal growth and structure parameters of (Ho, Tm):KGdW

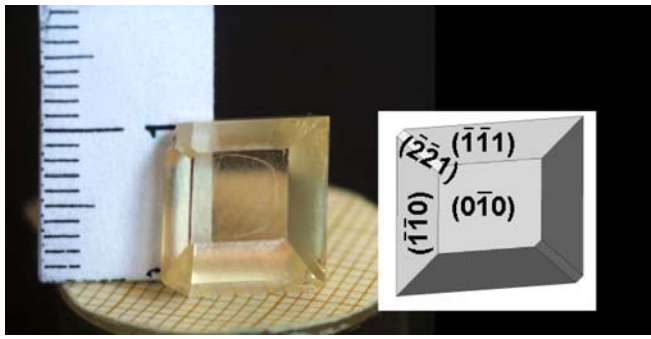
As we mentioned above, the single crystals reported in this paper were grown by the TSSG-SC method without pulling. The doping concentration range was designed to have a higher concentration of thulium, as a sensitizer ion, than holmium, the emitting ion. In one of the samples, the concentration of holmium was higher than the concentration of thulium. This was in order to compare the results with those of other samples.

Table 1 shows the results of the growth experiments. The axial temperature gradient in the solution was 0.08–0.125 K/mm. The growth rate for the codoped (Ho, Tm)

A	B	C	D	E	F	G	H	I	J	K	L	M
0.08	1.5	2.5	$b$	0.1/0.05	2/10	2.8614	130.06	None	8.3	5	13.9	1246.6
0.125	1.5	5	$b$	0.1/0.05	2/6	1.8766	134.04	None	7.4	4.8	10.3	1256.5
0.125	2.5	5	$b$	0.1/0.05	2/10	3.6044	163.84	None	11.2	4.2	13.6	1255.5
0.125	2.5	7.5	$b$	0.1/0.05	2/7	2.9718	185.74	None	8.8	5.7	13.1	1254.2
0.125	2.5	10	$b$	0.1/0.05	2/8	2.7902	155.01	None	9.4	6.0	12.0	1247.2
0.125	5	2.5	$b$	0.1/0.05	2/7	2.9871	186.69	None	10.9	4.8	11.3	1254.3

**A:** temperature gradient in the solution (K/mm). **B:**  $100 \times Ho_2O_3 / (Gd_2O_3 + Ho_2O_3 + Tm_2O_3)$  ratio in the solution, at.%. **C:**  $100 \times Tm_2O_3 / (Gd_2O_3 + Ho_2O_3 + Tm_2O_3)$  ratio in the solution, at.%. **D:** seed orientation. **E:** cooling rate, K/h. **F:** cooling interval, K. **G:** crystal weight, g. **H:** growth rate ( $\times 10^{-4}$ ), g/h. **I:** macrodefects. **J:** crystal dimensions along  $c$  direction, mm. **K:** crystal dimensions along  $a^*$  direction, mm. **L:** crystal dimensions along  $b$  direction, mm. **M:** saturation temperature, K

**TABLE 1** Experimental details of crystal growth



**FIGURE 1** Photograph of KGd<sub>1-x-y</sub>Ho<sub>x</sub>Tm<sub>y</sub>(WO<sub>4</sub>)<sub>2</sub> single crystal grown by TSSG-SC method

crystals was around  $130\text{--}190 \times 10^{-4}$  g/h, which takes into account an average cooling rate of  $0.06\text{--}0.07$  K/h. As this growth rate was lower than that for undoped KGdW, doping slowed the growth procedure. The crystals are macrodefect-free with good optical quality and are similar to the single-doped ones previously reported in the literature [27]. Figure 1 shows a photograph of (1.5% Ho, 1.5% Tm):KGdW (% of substitution of Gd<sub>2</sub>O<sub>3</sub> by Ln<sub>2</sub>O<sub>3</sub> in solution). These crystals show a similar morphology to that for undoped KGdW described in previous papers [27, 29] and faces (-111), (010), (130), (110) and (310). The appearance of faces (021) and (-221) seems to be favoured by the doping of KGdW.

The composition of the single crystals obtained was measured by EPMA. From these results and the solution composition, we determined the distribution coefficients of the holmium and thulium in KGdW. The distribution coefficients for Ho<sup>3+</sup> and Tm<sup>3+</sup> were close to unity. However, they were lower than for the single-doped Ho:KGdW or Tm:KGdW crystals. The two doping ions are in concurrence to enter the structure. Table 2 shows the EPMA results. The entrance of the holmium ions is more favoured than the entrance of the thulium ions. This is because the ionic radii of Gd<sup>3+</sup> and Ho<sup>3+</sup> are more similar than the ionic radii of Gd<sup>3+</sup> and Tm<sup>3+</sup>. However, the high distribution coefficient is important if homoge-

neously doped single crystals, which are useful for laser applications, are to be obtained. The detection limit of holmium in KGdW is 0.074% weight and the detection limit of thulium is 0.011% weight. All the measurements are up to these detection limits.

KGd(WO<sub>4</sub>)<sub>2</sub> crystals are monoclinic with space group *C2/c* and the unit-cell parameters for undoped KGdW are  $a = 10.652(4)\text{Å}$ ,  $b = 10.374(6)\text{Å}$ ,  $c = 7.582(2)\text{Å}$  and  $\beta = 130.80(2)$  [30] by single-crystal X-ray diffraction. To determine the effect of doping on the structure, we refined the unit-cell parameters of the undoped, single-doped and codoped KGdW by X-ray powder diffraction. We refined these by adjusting 13 parameters and with refinement reliability the Bragg *R*-factor was around 20. The results are shown in Table 3. There was an overall decrease of 0.094% for Ho-doped and 0.067% for Tm-doped crystal in relation to undoped KGdW (because of the low magnitude of the doping-induced lattice contraction, this contraction has not been taken into account for calculating the doping concentration in Table 2). In the codoped crystals, the overall decrease is 0.227% and 0.241% for KGd<sub>0.960</sub>Ho<sub>0.021</sub>Tm<sub>0.019</sub>W and KGd<sub>0.912</sub>Ho<sub>0.056</sub>Tm<sub>0.032</sub>W, respectively. We therefore expected a very slight decrease in the inter-atomic distance Ln<sup>3+</sup>–Ln<sup>3+</sup> in comparison with the undoped material, where the minimum distance between Gd<sup>3+</sup>–Gd<sup>3+</sup> ions was  $4.070(2)\text{Å}$  [31]. This short distance favours the energy transfer processes between the doping active ions.

#### 4 Absorption studies

We measured the absorption of Tm<sup>3+</sup> in the 700–900 nm (14 000–11 100 cm<sup>-1</sup>) pumping range, which corresponds to the bands associated with the Tm<sup>3+</sup> transitions from the <sup>3</sup>H<sub>6</sub> ground state to <sup>3</sup>H<sub>4</sub> and <sup>3</sup>F<sub>2</sub> + <sup>3</sup>F<sub>3</sub> at room temperature and in polarized light. As we mentioned earlier, the light was polarized parallel to the principal optical directions of the KGdW [28].

Figure 2 shows the spectra. The maximum cross section was  $8.0 \times 10^{20}$  cm<sup>2</sup> in the *E*/*N<sub>p</sub>* direction with a line width

Ho at.% in sol	Tm at.% in sol	<i>K</i> <sub>Gd</sub>	<i>K</i> <sub>Ho</sub>	<i>K</i> <sub>Tm</sub>	[Ho] (cm <sup>-3</sup> )	[Tm] (cm <sup>-3</sup> )	Chemical formula
1.5	2.5	1	0.77	0.78	$7.57 \times 10^{19}$	$1.20 \times 10^{20}$	KGd <sub>0.969</sub> Ho <sub>0.012</sub> Tm <sub>0.019</sub> (WO <sub>4</sub> ) <sub>2</sub>
1.5	5	1.02	0.85	0.71	$8.20 \times 10^{19}$	$2.27 \times 10^{20}$	KGd <sub>0.952</sub> Ho <sub>0.014</sub> Tm <sub>0.036</sub> (WO <sub>4</sub> ) <sub>2</sub>
2.5	5	1.02	0.88	0.76	$1.39 \times 10^{20}$	$2.40 \times 10^{20}$	KGd <sub>0.940</sub> Ho <sub>0.022</sub> Tm <sub>0.038</sub> (WO <sub>4</sub> ) <sub>2</sub>
2.5	7.5	1.03	0.85	0.73	$1.34 \times 10^{20}$	$3.47 \times 10^{20}$	KGd <sub>0.924</sub> Ho <sub>0.021</sub> Tm <sub>0.055</sub> (WO <sub>4</sub> ) <sub>2</sub>
2.5	10	1	1.08	0.98	$1.70 \times 10^{20}$	$6.18 \times 10^{20}$	KGd <sub>0.875</sub> Ho <sub>0.027</sub> Tm <sub>0.098</sub> (WO <sub>4</sub> ) <sub>2</sub>
5	2.5	1.01	0.87	0.82	$2.08 \times 10^{20}$	$9.90 \times 10^{19}$	KGd <sub>0.936</sub> Ho <sub>0.043</sub> Tm <sub>0.021</sub> (WO <sub>4</sub> ) <sub>2</sub>

**TABLE 2** Summary of the microanalysis results and elemental compositions of the samples used in this work. The distribution coefficient was calculated by  $K_{\text{Ln}^{3+}} = \frac{(\text{moles Ln}^{3+}/(\text{moles Ho}^{3+} + \text{moles Tm}^{3+} + \text{moles Gd}^{3+}))_{\text{crystal}}}{(\text{moles Ln}^{3+}/(\text{moles Ho}^{3+} + \text{moles Tm}^{3+} + \text{moles Gd}^{3+}))_{\text{solution}}}$ , where Ln<sup>3+</sup> can be Ho<sup>3+</sup> or Tm<sup>3+</sup>

	IR Ln <sup>3+</sup> (Å)	<i>a</i> (Å)	<i>b</i> (Å)	<i>c</i> (Å)	$\beta$ (°)	<i>V</i> (Å <sup>3</sup> )	[Ref]
KGdW	1.053	10.6890(6)	10.4438(5)	7.6036(4)	130.771(3)	642.83(4)	[30]
KGd <sub>0.952</sub> Ho <sub>0.048</sub> W	1.015	10.6884(7)	10.4380(6)	7.6024(4)	130.765(4)	642.40(3)	[30]
KGd <sub>0.959</sub> Tm <sub>0.041</sub> W	0.994	10.6868(6)	10.4389(6)	7.6010(4)	130.767(3)	642.22(4)	[30]
KGd <sub>0.960</sub> Ho <sub>0.021</sub> Tm <sub>0.019</sub> W	–	10.6814(4)	10.4358(4)	7.5970(3)	130.766(2)	641.37(4)	This work
KGd <sub>0.912</sub> Ho <sub>0.056</sub> Tm <sub>0.032</sub> W	–	10.6793(5)	10.4317(4)	7.5950(3)	130.764(2)	640.85(5)	This work

**TABLE 3** Unit-cell parameters by X-ray diffraction of the monoclinic double tungstates, *C2/c* spatial group

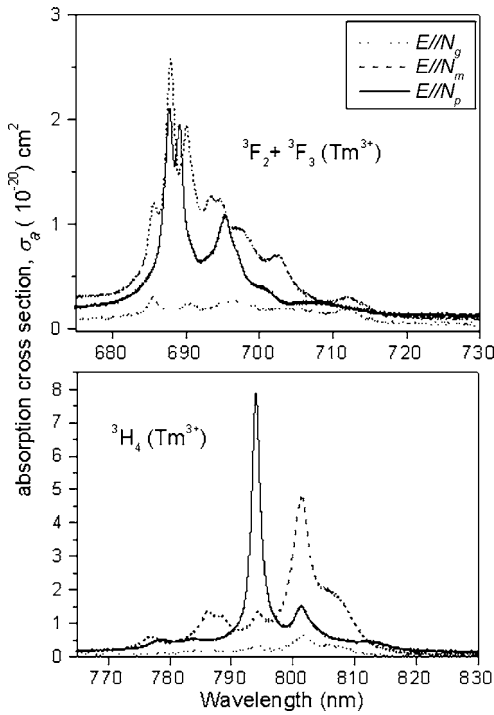


**FIGURE 2** Polarized room-temperature absorption of the  ${}^3H_4$  and  ${}^3F_2 + {}^3F_3$  excited states of thulium in the  $KGd_{1-x-y}Ho_xTm_y(WO_4)_2$  sample

of 1.7 nm at a wavelength of 794 nm. At 801 nm, the cross-section value was  $4.98 \times 10^{20}$  in the  $E//N_m$  direction with a line width of 3.2 nm (which is lower than (Ho, Tm):YAG crystal [5]). Both peaks can be pumped with the diode laser pumping source of AlGaAs, which is widely available. These absorption cross section values are similar to those for thulium single-doped KGdW.

We also measured, at room temperature, the absorption of the emitting holmium ion  ${}^5I_7$  level. From the values of the absorption, we can use the reciprocity method (RM) to calculate the theoretical emission cross section since 2-micron emission, the subject of this study, is a direct emission from the first excited level to the ground state,  ${}^5I_7 \rightarrow {}^5I_8$ . Figure 3 shows these results. The last three peaks of this emission band correspond to those determined in Ho:KGdW. For the codoped

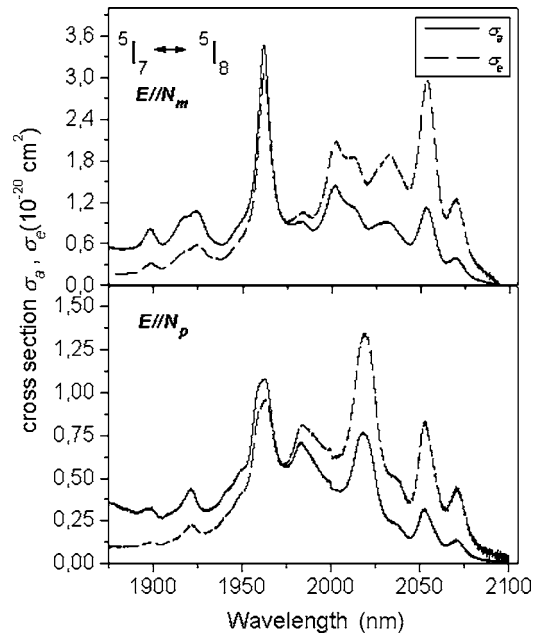


**FIGURE 3** Experimental absorption cross section of holmium ground state absorption  ${}^5I_7 \rightarrow {}^5I_8$  and calculated emission cross section in the 2-micron range

materials, the peaks are located at 2032, 2054 and 2070 nm. We should point out that at 2054 nm the emission cross section was around  $3 \times 10^{-20} \text{ cm}^2$  with  $E//N_m$ . Table 4 shows several values of this parameter. The value for (Ho, Tm):KGdW was higher than with the  $Ho^{3+}$  single-doped KGdW crystal [23] and several other hosts. It was also similar to that for Tm:KGdW,  $3.27 \times 10^{-20} \text{ cm}^2$  at 1.8  $\mu\text{m}$ , for which the laser action has already been achieved [32].

From the absorption values we can also calculate the radiative lifetime using the Weber expression [33]

$$A_{JJ'} = \frac{g_f 8\pi n^2 c}{g_i N \lambda^4} \Gamma,$$

where  $\Gamma$  is the integrated absorption. The calculated radiative lifetime is 11 ms. With regard to the Judd–Ofelt (J-O) calculated value for single-doped Ho:KGdW, 5.9 ms, a longer life-

(Ho, Tm):host	$\sigma_e Tm^{3+} {}^3F_4 \rightarrow {}^3H_6(\lambda_e)$	$\sigma_e Ho^{3+} {}^5I_7 \rightarrow {}^5I_8(\lambda_e)$	$\Delta E({}^5I_8)$	$\tau_{rad}$ (ms)	$\tau({}^5I_7)$ (ms)	$\sigma_e \times \tau$ ( $10^{-20} \text{ cm}^2 \text{ ms}$ )	[Ref]
(Ho, Tm):KGdW	–	2.94 ( $E//N_m$ , 2019 nm) 1.33 ( $E//N_p$ , 2054 nm)	–	–	2.1–5.7	6.2–16.5	This work
Ho:KGdW	–	2( $E \perp b$ , 2019 nm) 1.1 ( $E // b$ , 2019 nm)	319	5.8 (J-O)	–	–	[23]
Tm:KGdW	3.27( $E//N_m$ , 1834 nm) 1.64 ( $E//N_p$ , 1824 nm)	–	–	–	–	–	[32]
YAG ( $Y_3Al_5O_{12}$ )	0.22*(2011 nm)	0.98*(2100 nm), 0.9 (2091 nm)	535	7.8*	9.8*, 8.5	7.6*	[5, 42, 43]
YAP ( $YAlO_3$ )	0.50*(1936 nm)	1.30* (1980 nm)	499	8.1*	4.8*	6.2*	[42, 44]
LIF ( $LiYF_4$ )	0.40*( $E // c$ , 1980 nm) 0.33*( $E \perp c$ , 1902 nm)	1.84*( $E // c$ , 1980 nm) 0.99*( $E \perp c$ , 1988 nm)	315	15.6*	14.3*	26.3*	[42, 45]
BaYF ( $BaY_2F_8$ )	0.25*(1919 nm)	1.07*(2057 nm)	399	17.9*	13.2*	14.1*	[42, 46]
YVO <sub>4</sub>	2.60*( $E // c$ , 1805 nm) 1.73*( $E \perp c$ , 1804 nm)	2.6*( $E // \pi$ , 2038 nm) 1.8*( $E // \sigma$ , 2010 nm)	288	–	3.8*	9.88*	[47–49]

\* Single-doped values

**TABLE 4** Emission cross section values in  $10^{-20} \text{ cm}^2$  units in several solid-state materials

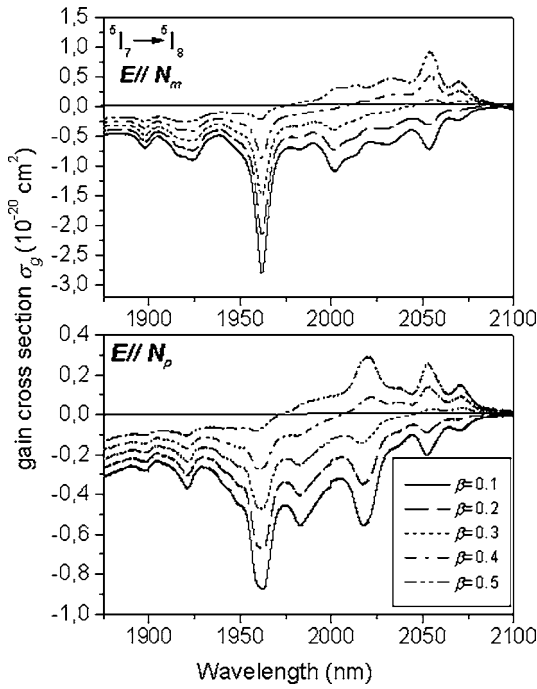


FIGURE 4 Effective emission cross section of 2-micron holmium emission for different  $\beta$  values in (Ho, Tm):KGdW

time of the emitting state will produce a greater electron storage in the codoped sample than with the single-doped sample. Further discussions about lifetime measurements are given below. We also used the expression  $\sigma_g = \beta\sigma_e - (1-\beta)\sigma_a$  to calculate the effective emission cross section (gain cross section) with  $\beta = 0.1, 0.2, 0.3, 0.4$  and  $0.5$  for  $E//N_m$  and  $E//N_p$  (Fig. 4). We can see that with  $\beta = 0.4$  we have a maximum effective cross section at  $2.054 \mu\text{m}$  of around  $0.9 \times 10^{-20} \text{ cm}^2$  for  $E//N_m$ .

A large Stark multiplet splitting of the ground state is most suitable for quasi-three-level lasers in order to obtain lower threshold population inversion. The highest sublevel of the ground state of holmium in KGdW was around  $320 \text{ cm}^{-1}$ , which means that the Stark splitting of holmium in the tungstate host is not very large compared to that of other well-known hosts (see Table 4).

In previous papers [34, 35], we published the splitting of the excited states involved in the energy transfer couple Tm–Ho in KGdW. We calculated that the energy shift was around  $380\text{--}690 \text{ cm}^{-1}$ . Taking into account these energy shifts, the phonons must play a role in the energy transfer phenomena. The phonon energies in this host are reported in [36, 37].

## 5 Luminescence results

### 5.1 Emission studies

To help interpret these results and discuss the excited state dynamics, the energy level scheme and possible energy transfer processes, which are important for thulium and holmium emission, are shown in Fig. 5.

The thulium pump process (1-GSA Tm), the energy transfer process from Tm to Ho (2-ET), the energy back transfer (3-BT) from holmium to thulium and the three cross-relaxation

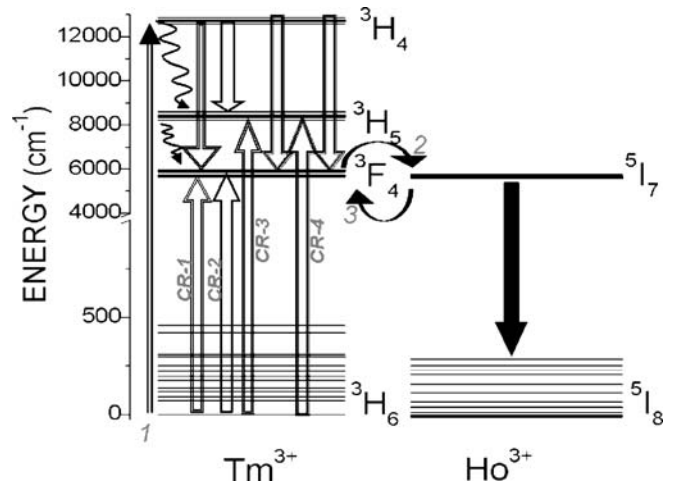


FIGURE 5 Sketch of holmium–thulium electronic states

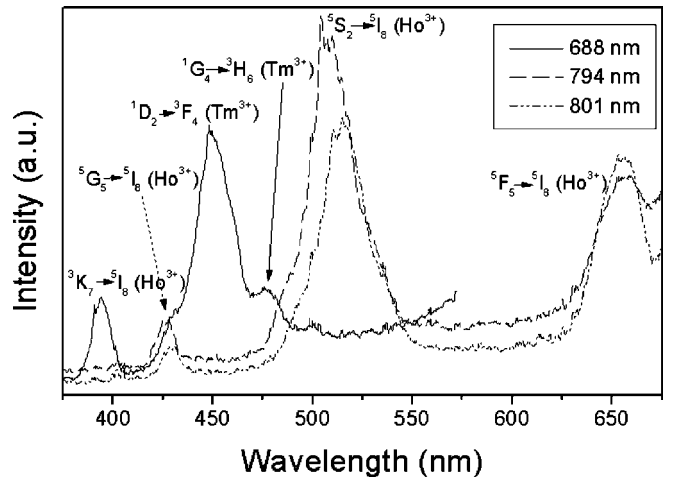


FIGURE 6 Visible emissions in (Ho, Tm):KGdW crystals

processes (CR): CR1 ( ${}^3H_4, {}^3H_6 \rightarrow ({}^3F_4, {}^3F_4)$ ); CR2 ( ${}^3H_4, {}^3H_6 \rightarrow ({}^3H_5, {}^3F_4)$ ) and CR3 ( ${}^3H_4, {}^3H_6 \rightarrow ({}^3F_4, {}^3H_5)$ ) [9], within the thulium energy levels, are indicated by arrows. Wavy arrows indicate the possible multiphonon relaxation pathways.

Figure 6 shows all the anti-Stokes visible emissions in the (Ho: Tm):KGdW system pumped at 688, 794 and 801 nm. Five visible channels can be observed:  $\lambda_e = 390 \text{ nm}$  ( $\text{Ho}^{3+}, {}^3K_7 \rightarrow {}^5I_8$ ),  $\lambda_e = 427 \text{ nm}$  ( $\text{Ho}^{3+}, {}^5G_5 \rightarrow {}^5I_8$ ),  $\lambda_e = 450 \text{ nm}$  ( $\text{Tm}^{3+}, {}^1D_2 \rightarrow {}^3F_4$ ),  $\lambda_e = 476 \text{ nm}$  ( $\text{Tm}^{3+}, {}^1G_4 \rightarrow {}^3H_6$ ),  $\lambda_e = 514 \text{ nm}$  ( $\text{Ho}^{3+}, {}^5S_2 \rightarrow {}^5I_8$ ) and  $\lambda_e = 655 \text{ nm}$  ( $\text{Ho}^{3+}, {}^5F_5 \rightarrow {}^5I_8$ ). These well-known visible emissions, reported in other materials such as Ho:KGdW [23], Tm:KGdW [24] and Tm:Yb:KYW [38], are the competitive processes for our emission at 2 microns.

The experimental luminescence peak in the region of 2 microns is shown in Fig. 7 for the  $\text{KGd}_{0.924}\text{Ho}_{0.021}\text{Tm}_{0.055}\text{(WO}_4)_2$  sample. This is promising for tunable emission due to its large width, which is broadened from 1650 nm to 2175 nm, and which is almost 525 nm of possible tunability. The peaks with maximum intensity are at 1836 nm and 2032 nm. The first broad peak belongs to thulium emission  ${}^3F_4 \rightarrow {}^3H_6$  in KGdW, which was reported in [39]. The second broad peak,

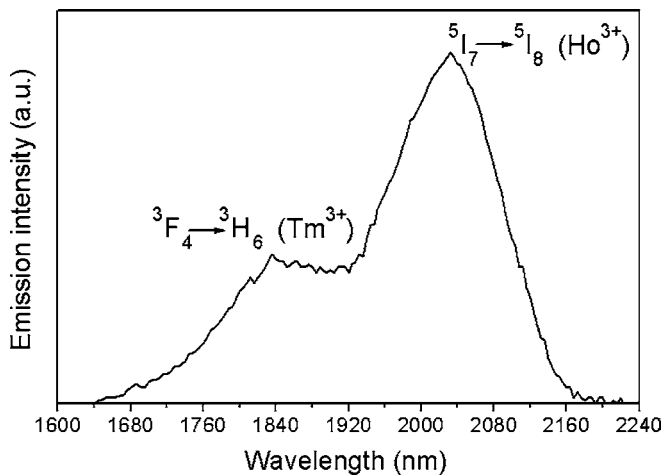


FIGURE 7 Room-temperature 2-micron emission in (Ho, Tm):KGdW crystals

which has a greater intensity, corresponds to the holmium transition  $^5I_7 \rightarrow ^5I_8$ , which supposedly includes the three emission maxima observed in the single-doped Ho:KGdW located at 2020 nm, 2051 nm and 2071 nm [24]. The fact that there was emission from both ions indicates that there was no complete energy transfer from  $\text{Tm}^{3+}$  to  $\text{Ho}^{3+}$ . This effect was also observed in (Ho, Tm):YAG [5].

## 5.2 Lifetime measurements

We measured the decay time of 2-micron emission and its dependence on holmium concentration and thulium concentration. Table 5 shows that these decay times were around 2.1–5.7 ms. On average, these were shorter than those in the bibliography for other hosts (see Table 4).

Processes of up-conversion and back-transfer, which depend on the absolute concentrations of  $\text{Ho}^{3+}$  and  $\text{Tm}^{3+}$  ions in the crystal, can modify the  $\text{Ho}^{3+}$  relaxation. Figure 8 shows the decay time as a function of the relative concentration of Ho ions. The increase in thulium concentration in the sample led to a fast decay of the 2-micron emission. Back-transfer phenomena may play an important role in this process. We should point out that the measured values have not been corrected for the different dimensions of the samples. Therefore, the decay time of the studied emission  $^5I_7 \rightarrow ^5I_8$ , with branching ratio equal to 1, is affected by the radiation trapping and total internal reflection (TIR) [40, 41]. The measured values cannot be taken as absolute values; but the tendency must be correct.

The laser threshold is proportional to  $(\sigma_e \times \tau)^{-1}$ . Table 5 shows these values for our samples taking into account the measured decay times.

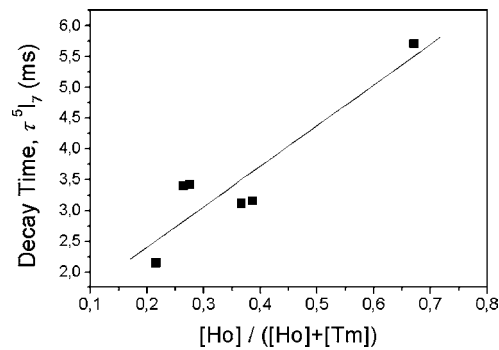


FIGURE 8 Decay time of the 2-micron emission and its dependence on holmium and thulium concentrations

## 6 Conclusions

Single crystals of (Ho, Tm):KGdW have been grown with high crystalline quality, without defects and in a broad band of doping ranges by the TSSG-SC method and using  $\text{K}_2\text{W}_2\text{O}_7$  solvent. The close distances of  $\text{Ln}^{3+}$ – $\text{Ln}^{3+}$  in the structure of this monoclinic compound assures an efficient energy transfer phenomenon between thulium and holmium.

The most important spectroscopic properties for modelling and understanding a future laser of 2 microns for the Ho–Tm system have been determined. These are absorption spectra for the diode pumping, emission cross section and lifetime of the upper state of the transition. A high absorption cross section at 801 nm and 794 nm of the thulium in the (Ho, Tm):KGdW samples will therefore allow an effective diode pumping of these samples. The maximum value of the cross section is  $8.0 \times 10^{20} \text{ cm}^2$  in the  $E//N_p$  direction with a line width of 1.7 nm at a wavelength value of 794 nm. At 801 nm, the cross-section value is  $4.98 \times 10^{20}$  in the  $E//N_m$  direction with a line width of 3.2 nm. The emission cross section for 2-micron emission calculated by RM at  $2.054 \mu\text{m}$  is around  $3 \times 10^{-20} \text{ cm}^2$  ( $E//N_m$ ). Finally, the measured decay times are in the 2–5 ms range.

The experimental fluorescence spectrum shows a broad emission around 525 nm, which is suitable for tunability of the emission. Also, the emission of  $\text{Tm } ^3F_4 \rightarrow ^3H_6$  is still present, so there is an important back-transfer. The back-transfer is also demonstrated by the decrease in the decay time when the thulium in the sample increases.

Additional properties, such as Tm–Tm cross-relaxation efficiency and net transfer from Tm to Ho, which depend on dopant concentration, are left for further studies.

**ACKNOWLEDGEMENTS** This work was supported by EU project DT-CRYS, NMP3-CT-2003-505580, by CICYT (Comisión Interministerial de Ciencia y Tecnología of the Spanish Government) under

	Ho/(Ho + Tm)	$\tau (^5I_7)$ ( $\lambda_{\text{exc}} = 801 \text{ nm}$ ) (ms)	$\sigma_e \times \tau$ ( $10^{-20} \text{ cm}^2 \text{ ms}$ )
KGd <sub>0.969</sub> Ho <sub>0.012</sub> Tm <sub>0.019</sub> W	0.387	3.15	9.45
KGd <sub>0.952</sub> Ho <sub>0.013</sub> Tm <sub>0.036</sub> W	0.265	3.39	10.2
KGd <sub>0.940</sub> Ho <sub>0.022</sub> Tm <sub>0.038</sub> W	0.367	3.11	9.33
KGd <sub>0.924</sub> Ho <sub>0.021</sub> Tm <sub>0.055</sub> W	0.276	3.41	10.2
KGd <sub>0.875</sub> Ho <sub>0.027</sub> Tm <sub>0.098</sub> W	0.216	2.14	6.42
KGd <sub>0.936</sub> Ho <sub>0.043</sub> Tm <sub>0.021</sub> W	0.672	5.70	17.1

TABLE 5 Experimental lifetimes of holmium  $^5I_7$  level and its dependence on thulium and holmium concentrations

the MAT-2005-06354-C03-02, MAT-04-20471-E and CIT-020400-2005-14 projects and by the Generalitat de Catalunya under project 2005SGR658. M.C. Pujol is supported by the Education and Science Ministry of Spain under the Ramón y Cajal program.

## REFERENCES

- 1 G.M. Hale, M.R. Querry, *Appl. Opt.* **12**, 555 (1973)
- 2 G.R. Osche, D.S. Young, *Proc. IEEE* **84**, 103 (1996)
- 3 A. Braud, S. Girard, J.L. Doualan, R. Moncorge, *IEEE J. Quantum Electron.* **QE-31**, 1880 (1995)
- 4 R.C. Stoneman, L. Esterowitz, *Opt. Lett.* **17**, 736 (1992)
- 5 T.Y. Fan, G. Huber, R.L. Byer, P. Mitzscherlich, *IEEE J. Quantum Electron.* **QE-24**, 924 (1988)
- 6 A.A. Kaminskii, L. Li, A.V. Butashin, V.S. Mironov, A.A. Pavlyuk, S.N. Bagayev, K. Ueda, *Japan. J. Appl. Phys.* **36**, L109 (1997)
- 7 A.A. Kaminskii, A.A. Pavlyuk, P.V. Klevtsov, I.F. Balashov, V.A. Berenberg, S.E. Sarkisov, V.A. Fedorov, M.V. Petrov, V.V. Lyubchenko, *Izv. Akad. Nauk SSSR Neorgan. Mater.* **13**, 582 (1977)
- 8 A.A. Kaminskii, A.A. Pavlyuk, *Izv. Akad. Nauk SSSR Neorgan. Mater.* **13**, 1541 (1977)
- 9 N.P. Barnes, E.D. Filer, C.A. Morrison, C.J. Lee, *IEEE J. Quantum Electron.* **QE-32**, 92 (1996)
- 10 C. Svelto, S. Taccheo, M. Marano, G. Sorbello, P. Laporta, *Electron. Lett.* **36**, 1623 (2000)
- 11 D.L. Dexter, *J. Chem. Phys.* **21**, 836 (1953)
- 12 T. Förster, *Faraday Discuss.* **27**, 7 (1959)
- 13 M. Inokuti, F. Hirayama, *J. Chem. Phys.* **43**, 1978 (1965)
- 14 T. Miyakawa, D.L. Dexter, *Phys. Rev. B* **1**, 2961 (1970)
- 15 M. Yokota, O. Tanimoto, *J. Phys. Soc. Japan* **22**, 779 (1967)
- 16 A.I. Burshtein, *Sov. Phys. JETP* **35**, 882 (1972)
- 17 S.A. Payne, L.K. Smith, W.L. Kway, J.B. Tassano, W.F. Krupke, *J. Phys. C: Condens. Matter* **4**, 8525 (1992)
- 18 N.P. Barnes, E.D. Filer, C.A. Morrison, C.J. Lee, *IEEE J. Quantum Electron.* **QE-32**, 92 (1996)
- 19 B.M. Walsh, N.P. Barnes, B.D. Bartolo, *J. Luminesc.* **90**, 39 (2000)
- 20 B.M. Walsh, N.P. Barnes, B.D. Bartolo, *J. Luminesc.* **75**, 89 (1997)
- 21 X. Mateos, V. Petrov, M. Aguiló, R.M. Solé, J. Gavalda, J. Massons, F. Díaz, U. Griebner, *IEEE J. Quantum Electron.* **QE-40**, 1056 (2004)
- 22 X. Mateos, V. Petrov, J. Liu, M.C. Pujol, U. Griebner, M. Aguiló, F. Díaz, M. Galan, G. Viera, *IEEE J. Quantum Electron.* **QE-42**, 1008 (2006)
- 23 M.C. Pujol, J. Massons, M. Aguiló, F. Díaz, M. Rico, C. Zaldo, *IEEE J. Quantum Electron.* **QE-38**, 93 (2002)
- 24 F. Güell, J. Gavalda, R. Sole, M. Aguiló, F. Díaz, M. Galan, J. Massons, *J. Appl. Phys.* **95**, 919 (2004)
- 25 S.N. Bagaev, S.M. Vatik, A.P. Maiorov, A.A. Pavlyuk, D.V. Plakushchev, *J. Quantum Electron.* **QE-30**, 310 (2000)
- 26 R. Solé, V. Nikolov, X. Ruiz, J. Gavalda, X. Solans, M. Aguiló, F. Díaz, *J. Cryst. Growth* **169**, 600 (1996)
- 27 M.C. Pujol, R. Solé, J. Gavalda, J. Massons, M. Aguiló, F. Díaz, *J. Mater. Res.* **14**, 3739 (1999)
- 28 M.C. Pujol, M. Rico, C. Zaldo, R. Solé, V. Nikolov, X. Solans, M. Aguiló, F. Díaz, *Appl. Phys. B* **68**, 187 (1999)
- 29 M.C. Pujol, M. Aguiló, F. Díaz, C. Zaldo, *Opt. Mater.* **13**, 33 (1999)
- 30 M.C. Pujol, R. Solé, J. Massons, J. Gavalda, X. Solans, C. Zaldo, F. Díaz, M. Aguiló, *J. Appl. Crystallogr.* **34**, 1 (2001)
- 31 M.C. Pujol, X. Mateos, A. Aznar, X. Solans, S. Surinac, J. Massons, F. Díaz, M. Aguiló, *J. Appl. Crystallogr.* **39**, 230 (2006)
- 32 V. Petrov, F. Güell, J. Massons, J. Gavalda, R.M. Sole, M. Aguiló, F. Díaz, U. Griebner, *IEEE J. Quantum Electron.* **QE-40**, 1244 (2004)
- 33 M.J. Weber, *Phys. Rev.* **4**, 9 (1971)
- 34 M.C. Pujol, C. Cascales, M. Rico, J. Massons, F. Díaz, P. Porcher, C. Zaldo, *J. Alloys Compd.* **323–324**, 321 (2001)
- 35 F. Güell, X. Mateos, J. Gavalda, R. Solé, M. Aguiló, F. Díaz, M. Galan, J. Massons, *Opt. Mater.* **25**, 71 (2004)
- 36 L. Macalik, J. Hanuza, A.A. Kaminskii, *J. Raman Spectrosc.* **33**, 92 (2002)
- 37 L. Macalik, P.J. Deren, J. Hanuza, W. Strek, A.A. Demidovich, A.N. Kuzmin, *J. Mol. Struct.* **450**, 179 (1998)
- 38 A.A. Demidovich, A.N. Kuzmin, N.K. Nikeenko, A.N. Titov, M. Mond, S. Kueckd, *J. Alloys Compd.* **341**, 124 (2002)
- 39 F. Güell, J. Gavalda, R. Sole, M. Aguiló, F. Díaz, M. Galan, J. Massons, *J. Appl. Phys.* **95**, 919 (2004)
- 40 D.S. Sumida, T.Y. Fan, *Opt. Lett.* **19**, 1343 (1994)
- 41 M.P. Hehlen, *J. Opt. Soc. Am. B* **14**, 1312 (1997)
- 42 S.A. Payne, L.L. Chase, L.K. Smith, W.L. Kway, W.F. Krupke, *IEEE J. Quantum Electron.* **QE-28**, 2619 (1992)
- 43 M.K. Ashurov, Y.K. Voronko, E.V. Zharikov, A.A. Kaminskii, V.V. Osiko, A.A. Sobol, M.I. Timoshechkin, V.A. Federov, A.A. Shabaltai, *Izv. Akad. Nauk SSSR* **15**, 979 (1979)
- 44 Y. Yang, J.A. DeLuca, *Appl. Phys. Lett.* **31**, 594 (1977)
- 45 N. Karayianis, D.E. Wortmann, H.P. Jenssen, *J. Phys. Chem. Solids* **37**, 675 (1976)
- 46 F. Johnson, H.J. Guggenheim, *IEEE J. Quantum Electron.* **QE-10**, 442 (1974)
- 47 M. Bass, L.G. DeShazer, U. Ranon, *Res. Dev. Tech. Rep.* **74**, 104 (1974)
- 48 W. Ryba-Romanowski, *Cryst. Res. Technol.* **38**, 225 (2003)
- 49 Y.K. Kuo, M. Birnbaum, *Appl. Opt.* **35**, 881 (1996)